
Evidence for synchronicity of lightning activity in networks of spatially remote thunderstorms

Yoav Yair*, Reuven Aviv, Gilad Ravid, Roy Yaniv and Baruch Ziv
The Open University of Israel, Ra'anana 43107 ISRAEL

Colin Price

Tel-Aviv University, Tel-Aviv 69978 ISRAEL

Submitted to
Journal of Atmospheric and Solar-Terrestrial Physics

September 2005

* Corresponding Author
Dr. Yoav Yair
Department of Life and Natural Sciences
The Open University of Israel
108 Ravutski Street
P.O. Box 808, Ra'anana
ISRAEL 43107

E-mail: yoavya@openu.ac.il

Abstract

Visual observations by space shuttle astronauts have described a phenomenon in which spatially distant thunderstorm cells seem to reciprocally "ignite" lightning flashes in a semi-cyclic sequence. Lightning occurring in one cell is immediately followed by lightning in other cells, separated by tens or hundreds of kilometers. We present quantitative analysis of lightning observations conducted within the framework of the MEIDEX-sprite campaign on board the space shuttle Columbia in January 2003 (Yair et al., 2003). Video footage of 6 storm systems with varying flash rates, which occurred over Africa, South America, Australia and the Pacific Ocean were analyzed. It is found that when the storm flash rate was high, lightning activity in horizontally remote electrically active cells became clustered, with bursts of nearly simultaneous activity separated by quiet periods. The recurrence time was ~ 2.5 seconds, close to the previously reported time delay between consecutive ELF transient signals in the Schumann resonance range (Füllekrug, 1995). We propose that this behavior is similar to the collective dynamics of a network of weakly coupled limit-cycle oscillators (Strogatz, 2000). Thunderstorm cells embedded within a mesoscale convective system (MCS) constitute such a network, and their lightning frequency is best described in terms of phase-locking of a globally coupled array (Kourtchatov et al., 1995). Comparison of basic parameters of the lightning networks with predictions of random-graph models reveals that the networks cannot be described by the classical random-graph model (Erdos and Renyi, 1960), but are more compatible with generalized random-graphs with a prescribed degree distribution (Newman et al., 2001) that exhibit a high clustering coefficient and small average path lengths. Such networks are capable of supporting fast response, synchronization and coherent oscillations (Lago-Fernandez et al., 2000). Several physical mechanisms are suggested to explain this phenomenon.

Keywords: Lightning networks;

1. Introduction

The proximity in time and space of consecutive lightning flashes in thunderstorms was first studied by Mazur (Mazur, 1982) who termed the phenomenon "associated lightning discharges". These flashes were reported to occur in multi-cell storms, where several electrically active cells (EACs) co-exist in the same mesoscale region. VHF radar observations showed that lightning echoes from discharges follow one another within a time interval typical of a multistroke cloud-to-ground (CG) flash, but are spaced in range by several km. *Mazur* (1982) chose the maximum time interval of 200 ms between single echoes in analogy with that for the between-stroke interval of multistroke flashes, and used statistical methods to disprove the null hypothesis that these associated discharges were merely a pooled output of randomly occurring flashes. These associated discharges were different from CG strokes in that they were separated in space and lacked a common discharge path. He concluded that an association between flashes is the triggering of one flash by another flash, separated spatially from it, and suggested that the interdependence of the electric field within neighboring EACs may be the responsible mechanism.

Reports of a similar phenomenon, but on a larger scale, were obtained from astronauts in manned space missions, compiled by *Vonnegut et al.*(1985). They quote

astronaut Edward G. Gibson who flew on the Skylab 4 mission in November 1973. After noting the fact that lightning was occurring simultaneously or almost simultaneously over wide areas and large distances, he used the phrase "sympathetic lightning bolts" to describe the repeated sequences of lightning activity. Gibson claimed that tens of lightning flashes were occurring almost together after periods of calm, and then the activity subsided for several seconds, only to resume again "in all location". Astronaut Richard H. Truly, who flew the space shuttle missions STS-2 and 8, reported two separated areas of frequent lightning in the Amazon basin that appeared "to be talking to each other". These and other reports suggested the existence of a possible coupling between widely separated lightning events and were among the drivers to perform space shuttle observations of thunderstorms, in what was later called the Mesoscale Lightning Experiment (MLE). The results from the MLE were discussed by Vonnegut et al. (1985) and were later used to verify the discovery and the existence of sprites and Elves (Boeck et al., 1998). *Vonnegut et al.* (1985) analyzed the video images taken by the shuttle crews of STS-2, 4 and 6 missions (November 1981, June 1982 and August 1983, respectively). The manual analysis of 8 lightning events focused on the extent, speed of propagation and patterns of luminosity, and provided evidence for at least one episode of simultaneous lightning separated by 82 km. The authors suggested that the manner of luminosity pattern development as observed from space is caused by the release of electrical energy in one portion of the cloud, which eventually triggers the development of a new breakdown process in another part. This limited study has not supplied a conclusive mechanism to explain the observations.

The three shuttle video excerpts posted on the GHCC web-site (<http://www.ghcc.msfc.nasa.gov/skeets.html>) are good examples of mesoscale lightning activity as observed from Earth orbit, and indicate that lightning occurs in what appears to be a cyclic pattern. These anecdotal sequences cannot divulge if this is a random or an organized process. The purpose of the present study is to perform a quantitative analysis of this phenomenon as it appears in space shuttle videos and to discuss its possible source.

2. Network structure and synchronicity in naturally occurring coupled systems

There is now a considerable body of theoretical and experimental research that relates the properties of complex dynamical phenomena to those described by network phenomenology. Examples for the usage of network models can be found in solid-state physics (*Weisenfeld*, 1996), molecular biology (*Milo et al.*, 2002), ecology (*Williams and Martinez*, 2000), metabolic processes (*Jeong et al.*, 2000) and climate (*Tsonis*, 2004). In the broad sense, a network is a system composed of several separate interacting entities, relating to each other in different modes with varying levels of complexity. Each member of the network is called a "node" that may or may not be connected to the other nodes of the network, in a fixed or evolving (dynamic) topology. The present study of thunderstorms is obviously more in the realm of dynamic networks, where the interaction between the multiple nodes is time-dependant.

In his extensive review, *Strogatz* (2001) offers rules-of-thumb that describe the impact of network structure on the collective dynamics of arrays of coupled limit-cycle oscillators. He quotes the early work on biological oscillators by *Winfree* (1967), that showed how a system of nearly identical, weakly coupled limit-cycle oscillators exhibit

incoherent behavior when the coupling is small compared to the variance of natural frequencies. However when the coupling increases beyond a certain critical threshold, a cluster of oscillators can suddenly self-synchronize. *Kuramoto* (1984) used a Lorentzian probability distribution for the natural frequencies and amplitudes of the oscillators and showed that the transition to a synchronized state depends on the order parameter (R). Once the coupling strength exceeds a certain threshold, the system exhibits a phase transition: some of the oscillators spontaneously synchronize while others remain incoherent (Pérez et al., 1996). *Kurtchatov et al.* (1995) presented an analytical study and numerical simulation of the dynamic behavior of an optically globally coupled laser array possessing time-independent spread eigenfrequencies. They showed that the system can transit between phase-locked and unlocked regimes, and also identified an effect they named "cooperative field phase locking". According to their analysis, this effect takes place regardless of the large spread of eigenfrequencies because of the short duration of the laser pulses. This behavior persists also in the case of a small number of array elements. Similarly, *Strogatz* (2001) showed that spontaneous synchronization can emerge in a network of non-identical oscillators with distributed natural frequencies (Fig.2 *ibid*). Starting from a random initial condition, the oscillators rapidly self-organize and are pulled toward the mean field that they generate collectively, such that their phases lock and the fastest oscillators dominate.

All the network topologies discussed above are completely regular, that is, the degree - the number of neighbors of a node - is homogeneous. Several authors extended their investigation into systems connected by general graph, with degree distribution which is not necessarily homogeneous. It has been shown (Atay et al., 2005) that prescribing a degree distribution does not suffice to characterize the synchronization of oscillator networks. *Lago-Fernandez et al* (2000) investigated the role of different degree distributions in the dynamics of a network of Hodgkin-Huxley neurons by computer simulations. They found that regular networks produce coherent oscillations, but in a slow time scale, because the input from a node to others needs to propagate through long paths. On the other hand randomly generated networks give rise to fast response, because the average path length between nodes is relatively short. But randomly generated networks produce no coherent oscillations, because a specific node receives signals from neighboring nodes that do not necessarily communicate among themselves. The middle course is obtained by decreasing the path length of regular networks by inserting randomly generated shortcuts between far away nodes; this enables fast synchronicity (this is the small-world topology (Watts, 1999)). Numerical analysis of generic network model of oscillators linearly and symmetrically coupled provided similar results (*Barahona and Pecora*, 2002). These results agree with earlier conjecture made by *Watts and Strogatz* (1998).

Following this line, we propose that the co-occurrence of lightning flashes in spatially distant electrically active cells is not a fully random process (although it certainly has a random component), and that it reflects some intrinsic network behavior, which may be a reflection of a physical mechanism. Note that the large distances between the observed flashes exclude the possibility that what we view from space as simultaneous flashes are merely different parts of the same lightning channel being illuminated at different times as the discharge process progresses.

3. Characteristics and models of networks

Before dwelling into dynamics we need to explore the possibility that the detected phenomenon is merely a manifestation of the randomness in the timing of the lightning activity of vastly separated thunderstorm cells. To do this we model the lightning phenomena as a stochastic network of electrically active cells (EACs). An EAC i is linked to an EAC j if a lightning flash in EAC i was followed by a lightning flash from EAC j within a certain time window τ .

Any two nodes of a network are a dyad, which can be in one of three states: fully connected (reciprocal), semi-connected (one direction only, 2 options) and null (not connected). The abundances of dyads in the different states are defined as the dyad census.

Similarly, any three nodes network form a triad, which can be in one of 16 states (Milo *et al.*, 2002), from completely unconnected (3 isolated nodes) to the fully, reciprocally connected (3 nodes with 6 directed links). The possible states are denoted by a well known scheme (Wasserman and Faust, 1994) used in social network analysis. The abundances of triads in the different states are defined as the triad census.

The over-all network structure is sometimes described by its characteristic path-length L and the clustering coefficient C . These two parameters quantify the structural properties of networks and help distinguish between their various types (Watts and Strogatz, 1998). The path length L is the average number of links that are needed to connect any two nodes in the network. The Clustering Coefficient (C) is a measure of local clustering (Newman, 2003a). Specifically if a node i is linked to k_i neighbors, then its clustering coefficient C_i is the ratio between the actual number of links between these neighbors and the maximal number of such links, $k_i(k_i - 1)$. The network clustering coefficient is the average of C_i over all i . As noted in section 2, these two characteristics seem to be related to the phenomena of fast synchronicity in dynamical networks.

There are several models that describe network topologies. The first is the classical Erdos-Renyi (ER) Random Graph model (Erdos and Renyi, 1960). This model describes networks with g nodes that are linked at random. The model depends on a single input parameter, the link probability p ; this is the probability of any given node to be connected to another node. Alternatively, the average degree $\langle k \rangle$ is used instead, a factor that reflects the number of links each node in the network has. It is well known (Albert and Barabasi, 2002; Newman, 2003b) that some features of this model, in particular the short average path length between nodes are compatible with observed features of many real natural networks. On the other hand other features of the ER model, notably the small clustering coefficient and the nearly homogenous degree distribution, deviate significantly from the observed characteristics of many networks (Albert and Barabasi, 2002; Newman, 2003b). To better address this situation, it is common to use two variants of the generalized random graph model. The Fixed Degrees (FD) random graph model (Molloy and Reed, 1995; Newman *et al.*, 2001) describes an ensemble of networks with g nodes that connect at random subject to a predetermined, fixed degree distribution. Hence the model depends on g input parameters – the fractions of nodes with degrees equal to 0, 1, ... $g-1$. The second variant is the Fixed Degrees and Reciprocities random graph (FDR) model (Snijders, 1991) which describes an ensemble of networks with g nodes that connect at random, subject to the conditions that the degrees as well as the dyad census are held fixed.

In order to identify the nature of the randomness of the lightning phenomenon we compared the above mentioned characteristics of the observed lightning networks with the predictions of the ER, FD and FDR random graph models. In section 5 we present the analysis for the lightning network for the orbit 67.

4. The MEIDEX lightning data

The data used in this research is the result of a series of lightning observations, performed within the framework of the Mediterranean Israeli Dust Experiment (MEIDEX) Sprite-campaign conducted in January 2003 on board the space shuttle Columbia (Yair et al., 2003). When searching for Transient Luminous Events (TLEs; see (Israelevich et al., 2004; Yair et al., 2004; Yair et al., 2005), we noticed the semi-cyclic pattern mentioned by Vonnegut et al. (1985), and clearly observed how distant thunderstorm cells seemed to "ignite" each other in a repeating sequence, with periods of quiet and diminished activity in between active ones. Lightning occurring in one region were immediately followed by lightning in other regions, separated by tens or hundreds of kilometers. The time delay of the onset of a visible flash in one thunderstorm from that of the following flash in the distant active cell varied from several tens of milliseconds to seconds. The gaps and recurrence of lightning activity was also quite clear from the video images, and prompted us to perform a quantitative estimate of this Mesoscale phenomenon and to suggest possible generating mechanisms.

The MEIDEX payload consisted of two bore-sighted cameras, a Sekai wide-FOV color camera for target acquisition, and a Xybion IMC-201 multispectral radiometric science camera, equipped with a rotating filter wheel (5 Hz) which had 6 narrow-band filters. The Xybion FOV was rectangular, 10.76° vertical and 14.04° horizontal (diagonal 17.68°), with a 486×704 pixel CCD, where each pixel corresponds to $1.365 \cdot 10^{-7}$ steradian. The camera footprint, superposed on the ground, covered an area of $\sim 1148 \times 465$ km, where the closest range to the shuttle was 700 km and the Earth's limb was ~ 1900 km away. The video format was NTSC at 30Hz (33.3 ms/frame), recorded internally in the payload canister on 3 digital tapes and also in the shuttle crew-cabin for backup. Some of the data were also transmitted to the ground and saved. In all, the MEIDEX-sprite campaign consisted of night-time limb imaging by the Columbia astronauts in 24 dedicated orbits. Each observation window consisted of ~ 25 minutes and the camera was commanded toward visible lightning activity centers. Data from 21 orbits was saved on the ground, with ~ 6 hours of video. Approximately 1/5 of the recorded data contained actual stormy regions, most of these in SE-Asia, Australia, Africa and the Pacific and Atlantic oceans. Admittedly, with the shuttle moving at 8 km s^{-1} the total observation time of a typical Mesoscale Convective System ($\sim 20,000 \text{ km}^2$; (Zipser, 1982)) is limited to only several minutes. However, in the Southern Hemisphere summer storms that we observed the flash rate was almost always higher than 25 flashes per minute, a fact that allowed performing the analysis on a sufficiently large number of flashes.

4.1 Data generation

We recorded the flashes occurring in any single video frame, and identified the Electrically Active Cells (EACs) that co-existed within each storm system. The movement of the space shuttle and camera pointing maneuvers performed by the

astronauts necessitated a very meticulous tracking of the EACs as they changed location within successive video frames, until finally disappearing behind the horizon or outside the camera FOV. An example of a lightning field showing simultaneous flashes is shown in Figure 1. The outlines and locations of each EAC were marked and the time series of flash occurrences and durations were registered. The time resolution of the analysis is dictated by the video frame rate, and hence has the accuracy of 33 ms. This frame-by-frame analysis enabled identifying the dominant EAC that had the highest flash rate, and the time series of that EAC was then cross-correlated with those of the other cells that were visible in the image. The relative distances between neighboring EACs were calculated based on their location in the image and the geometry of the observation. Since the pointing accuracy of the camera during the observations was $\sim 1^\circ$, the resulting error is range dependant and estimated to be < 50 km.

----- Figure 1 about here -----

Since the primary objective of the MEIDEX-sprite campaign was to observe mesospheric transient luminous events, most observations were conducted with the rather narrowband filters #5 (665 ± 50 nm) and #6 (860 ± 50 nm). The camera gain was set to 80-90% in order to capture faint TLE's. This resulted in lightning flashes saturating the camera and appearing as white patches in the video image. The duration of each luminous event in the video data depends on the viewing geometry, cloud obscuration and lightning-source intensity. The analysis performed by *Bocippio et al.* (2000) to assess the performance of the Optical Transient Detector (OTD) satellite, showed that between 46 to 69 percent of cloud-to-ground (CG) flashes were detected, with a slightly better performance for intra-cloud flashes (IC). We cannot quantitatively estimate the detection efficiency of lightning flashes by the MEIDEX instrument, nevertheless the superior sensitivity of the camera and the lower orbital altitude of the space shuttle seem to guarantee an equal or better detection rate.

We analyzed 7 video segments of major storm systems tracked by the shuttle astronauts. All these storms displayed the above mentioned phenomenon to some degree. Here we present the results of three systems with different flash rates - high, medium and low (these categories were based on the flash rates cited by (Rakov and Uman, 2003); Table 2.2 *ibid.*). The UT time marks the beginning of the observations, details of which are summarized in Table 1. For each visible flash, we registered the time, duration and the identity of the parent cell. This data-base of time series documents the lighting activity of the entire system.

4.2 Orbit 67 – January 20th 2003, 19:14 UT

This was a high flash-rate storm that occurred north-east of New-Zealand, over the Pacific Ocean. The observation lasted 152 s and recorded a total of 379 flashes (average flash rate of 150 min^{-1}) located within 13 distinct EACs. The time series of lightning activity and flash durations is shown in Figure 2a. At first glance, the overall pattern of the flash occurrence appears as a random distribution and may be considered to be the consequence of a pooled output of unrelated events (*Mazur*, 1982). A closer look reveals clustering of several consecutive flashes in different cells occurring successively in short time intervals, with longer breaks between the clusters without any flash. Note

that this statement is true for those EACs that were inside the camera FOV at the time of the observation.

----- Figures 2a, 2b about here -----

We detected 9 distinct clusters of lightning activity with an average duration of 9.7 s containing 23 flashes per cluster on average. The average interval between subsequent flashes within such a lightning cluster was 0.41 s, while the average "dead time" with no lightning activity between clusters was 2.48 s. The Fourier analysis (Fig 2b) shows that the dominant time interval between bursts of activity is ~2.5 s. Out of 379 flashes, 272 were concentrated in clusters, the rest seemed to be occurring singularly. There were 79 video frames that contained 2 or more simultaneous flashes in separate and distant EACs. This shows that in 20% of the events the flashes in clusters occurred within 33ms or less from each other. There were two distinctly active cells: #2 (122 flashes) and #4 (89 flashes), and all the other cells displayed a lower flash rate. Distances between the most active EACs to the other, less active ones, ranged from 100 to 430 km.

4.3 Orbit 87 – January 22nd 2003, 01:29 UT

This storm exhibited a medium flash rate, and occurred over the Congo basin in central Africa. The observation lasted 202 s and recorded a total of 274 visible flashes (average flash rate of 81 min⁻¹), that were concentrated in 9 distinct EACs (see the example of 3 distinct cells in Figure 1). We identified 23 flash clusters, in which there was an average of 12 flashes and an average duration of 5.26 s. The average interval between subsequent flashes within the same lightning cluster was 0.47 s. The average "dead time" was 3.15 s. Out of 274 flashes, 268 were concentrated in clusters, and only 6 appeared separately. There were 39 video frames that contained 2 or more simultaneous flashes in separate and distant EACs (14%). There was one dominant cell (#4) that generated 121 flashes during the observation window. The distances between this EAC to the cells ranged from 35 to 750 km.

4.4 Orbit 48 – January 19th 2003, 14:49 UT

This low flash-rate storm occurred over the Maritime Continent, to the east of Indonesia and over the Pacific Ocean. The observation lasted 165 s and recorded a total of 76 flashes (average flash rate of 27.6 min⁻¹), concentrated in 4 distinct EACs. There were 15 clusters of lightning activity, with an average duration of 3.16 s and a time separation between bursts of activity of 6.43 s. The average flash number in a cluster was 4. Unlike the higher flash-rate storms, this storm displayed only weak clustering where a significant number of flashes (19 out of 76) appeared to be isolated, namely, detached from any cluster. This storm system did not exhibit the organized activity observed in other storms, a fact that can be explained by the decaying stage of the system and the weakening convection.

5. Analysis of lightning networks

In this study we analyzed the highest flash rate storm, observed during orbit #67. A computer program scanned the Excel spreadsheet representation of the lightning

sequence (visually presented in Fig. 2a), identifying EACs with co-occurrences of flashes within a prescribed time-window. As an example, the orbit #67 lightning sequence with a time window of $\tau = 0.01$ s is presented in Figure 3. In this figure, the observed network of EACs is presented by a topographic like "centrality map" - the higher connectivity EACs are closer to the center. Note that the emergent network is highly clustered, with a central clique of nodes that are connected to almost all other nodes.

----- Figure 3 about here -----

As mentioned in section 3, the nature of the randomness of the lightning phenomena is revealed by comparing a set of characteristics of the observed lightning networks with the predictions of the ER, FD and FDR random graph models described above. When comparing predictions of random graph models with an observed real-world network, the input parameters for the simulations are estimated from the observed network. In the following sub-sections we perform this analysis to the lightning network for the orbit 67.

5.1 Dyad census

Consider first the ER model of a network with g nodes; each node has $g-1$ possible neighbors, each of which has a probability p to be linked with the focus node. In the ensemble created by the ER model, $(g-1)p$ nodes will be linked, on the average, to any node (Bollobas, 2001) ; this is the ensemble average degree: $\langle k \rangle = (g-1)p$. Hence, for a given average degree $\langle k \rangle$ the link probability is $p = \langle k \rangle / (g-1)$. We will estimate $\langle k \rangle$ by the average degree of the observed network.

There are no explicit formulas for the distributions and expected values of the dyad states in the ensemble generated by the generalized random graph models. We obtain estimates of these by a simulation. All the simulations in this study were done by the Netminer package (NetMiner CYRAM Co. Ltd, 2004). For each lightning network and each time-window τ we generated a sample 500,000 simulated networks. The expected values and accumulated probabilities for the observed numbers of dyads in the three states are derived from these ensembles. Figure 4a and 4b present the abundance of reciprocal and null dyads, respectively, for the orbit 67 for 4 time-windows. In these figures the observed abundances are compared with the expected numbers predicted by the ER and the Fixed Degrees random graph models. It is clear that the observed values deviate considerably from the ER predictions. In particular, the observed number of reciprocal dyads, which is clustering at the dyad level, is much higher than the prediction of the ER model. On the other hand, the predictions of the Fixed Degrees Random Graph model agree well with the observed values. Using the probability distributions we statistically confirm both of these conclusions with a significance level of 1%.

----- Figures 4a, 4b about here -----

5.2 Triad census

We calculated the triad census for lightning network orbit 67, at 4 time-windows. In addition, for each observed network we created two ensembles of 500,000 generalized random graphs (one ensemble for each of the FD and FDR models). From the ensembles we computed the expected triad census. The results, plotted in Figure 5, show that the observed values deviate considerably from the values predicted by the FD model, but

agree well with the predictions of the FDR model. This suggests that the triad census is compatible with the generalized graph model, and that the deviations are an artifact of the high level of reciprocity in the lightning networks (Snijders, 1991).

----- Figure 5 about here -----

Gaining confidence that the lightning network was not generated by a pure (ER) random process but might be compatible with generalized graph model, we now turn to close examination of the two characteristics that seem to be related with fast synchronization, the clustering coefficient and the average short path (Lago-Fernandez et al., 2000)

5.3 Clustering coefficient.

In the ER model the average fraction of any set of neighbors that are connected is p , the link probability. Hence, C_{rand} of a network is $p = \langle k \rangle / (g-1)$, where $\langle k \rangle$ is the average degree. The probability distribution and the expected values of C in the FD and FDR models were obtained by numerical simulations. In Figure 6 we compare the observed values of the clustering coefficients of the lightning network of orbit 67 in 4 time-windows with the expected values predicted by the random ER and the two generalized random graph models. Again it is clear that the values of the ER model deviate considerably from the observed values, whereas the predictions of the FD and FDR models fits very well with the observed values (and with each other). The latter conclusion is statistically confirmed with a significance level of 1%.

----- Figure 6 about here -----

5.4 Average path length

The average path length is the average over all pairs of nodes of the shortest path (measured in units of links) between the pairs. The lightning networks exhibit, like many other networks, short average path length (about 1.5). “Short” in this context means comparable with the prediction of the ER model, which is of the order of $\log(g)/\log(\langle k \rangle)$ (Albert and Barabasi, 2002). Again, the results of the FD and FDR models were derived by numerical simulations. In Figure 7 we compare the observed values of the average path length of the lightning network in the orbit 67 data, for 4 time-windows, with the predicted values of the ER model and the two generalized random graph models. The later values were derived from ensembles of 500,000 simulated networks per observed network, per model. In all cases the average path length is short. Again, the agreement between the observed values and the predictions of the FD and FDR models is very good, with a significance level of 1%.

----- Figure 7 about here -----

From the observations thus far we can conclude that the ER model cannot adequately describe the lightning network, for the same reason that it cannot describe numerous other real networks: the ER model predicts relatively low local clustering, at both the dyad and the triad levels, whereas real networks are heavily clustered (at the

local level). Our analysis suggests that the two generalized random graph models (FD and FDR) properly describe the observed lightning networks.

6. The physical mechanism of lightning networks

Our results suggest that thunderstorm cells embedded within a mesoscale convective system might be modeled as a network of non-identical oscillators, where each electrically active cell goes through the familiar evolutionary cloud growth-decay cycle while generating lightning discharges at a changing rate. Each new cumulonimbus cloud that becomes mature turns into an electrically active cell (EAC) and becomes a node in the network. Obviously, the coupling between the various points in this lightning network does not necessitate a physical contact between the cells, as will be discussed below. The topology of the lightning flash network is compatible with generalized random models with prescribed degree distribution, and it is characterized by a high clustering coefficient and short average path lengths. As such it is capable of supporting fast synchronization (Lago-Fernandez et al., 2000; Strogatz, 2000). The question is, then, what could be the physical mechanisms underlying the dynamics of the lightning flash network.

The clustering of lightning discharges has been detected in sferics signals in the low frequency range (10 Hz-60 kHz) and in Schumann resonances in the ELF domain (0.1-20 Hz). It is well known that natural radio noise below 100 MHz is impulsive and mostly created by lightning activity. *Füllekrug* (1995) recorded the magnetic field components in the lower ELF range at a station in Göttingen (Germany). The recorded time series shows the recurrence of intense flashes exciting the Schumann resonance in the earth-ionosphere cavity. The distribution of time delays between two consecutive signals was best explained by a normally random number distribution, except for a conspicuous maximum at a time delay of 1.95 s (Fig. 3 *ibid.*). The suggested mechanism inducing this recurrence behavior was by whistler excitation (*Armstrong*, 1987). The propagation of whistlers produced by a lightning flash along the lines of the magnetic field leads to reflection by the ionosphere at the opposite hemisphere, and this travel time is manifested in the detected delay of the next lightning signal arriving from a specific location. Such a mechanism would probably not be relevant to tropical storms in the equatorial regions, where the magnetic field lines are parallel to the earth's surface.

A second explanation arises from the fact that lightning discharges re-arrange the spatial distribution of charges within thunderstorms and hence affect the strength and shape of the electric field within the storm and in the outside surrounding. There is a considerable body of theoretical studies that discuss propagation effects of the lightning fields (*Rachidi et al.*, 1996; *Ming and Cooray*, 1994; *Cooray and Ming*, 1994), but most of these studies concentrate at ground level. For example, *Lin et al.* (1979) reported that peak fields are attenuated 20 percent propagating over soil over a distance of 200 km. A much lesser attenuation is expected when the propagation is over salt water. The electromagnetic energy propagating from the discharge channel is reflected from the ground and from the ionosphere, and these waves can, in principle, interfere and produce minima and maxima in the electric field. Local maxima may briefly enhance ionization within neighboring thunderclouds and expedite the discharge process, which would have occurred naturally but at a slower pace.

A similar reasoning was used by *Cho and Rycroft* (2001) to investigate the ionization created in the mesosphere leading to the formation of sprites and Elves. They used a numerical model to show that constructive interference between waves (generated by an intra-cloud discharge) reflected from the ground and the ionosphere, leads to creation of localized peaks of electron densities between 75 and 85 km. These peaks can serve as starting, or seeding, points for columniform sprites provided the quasi-electrostatic electric field, generated by a positive cloud-to-ground flash, is strong enough. In an analog manner, interference between propagating EM waves generated by a cloud-to-ground discharge can produce local enhancement of the electron concentration within mature thunderclouds that are located far from the parent lightning. Such a mechanism had not been modeled yet.

It has already been suggested by *Inan et al.* (1996) that the EMP from a CG can induce ELVES in the mesosphere. This pulse can be bounced back from the ionosphere and create constructive interference that will enhance ionization and the local electric field. However, any mechanism that relies on the propagation of the EMP pulse which follows a CG discharge would be good to explain only those synchronous events that were recorded on the same video frame. That is because EMP travels much faster than one video frame (0.033 s) so that even active cells at ~500 km separation would still have to appear in the same image. Indeed, the data shows that 20% of the flashes in orbit 67 and 14% of those observed in orbit 87 occurred in the same frame.

One additional possibility to explain flash synchronicity is related to the static electric field generated by large pockets of charge in thunderclouds. A point charge at height H will generate a maximum field at a horizontal distance D from the point charge, when $H/D \sim 1$. If the point charge is found at 20 km altitude (positive charge in tropical thunderstorms), then the induced field will maximize ~ 20 km away from the storm. Hence, after a large negative CG, the remaining positive charge in the cloud acts as a point charge. This region of charge induces a large electric field that has a maximum at a distance from the storm that is similar to the height of the charge center. Therefore after a CG lightning discharge, an enhanced electric field is felt at a distance of 20 km from the parent stroke. These enhancements of the electric field may trigger remote regions in the storm that are already close to breakdown.

7. Summary

The apparent synchronization in lightning activity in spatially remote thunderstorm cells is a fact reported by many observers. Clearly, the vantage point from space offers a broader view and enables to track the mesoscale behavior of active cells. Our quantitative study demonstrates that the system behavior is not wholly random and displays some level of organization.

There are still unknown factors concerning the onset of the electrical breakdown within maturing cumulonimbus clouds that leads to a lightning discharge. *Gurevich et al.* (1999) suggested that cosmic ray showers are the triggering mechanism that drives the electron avalanche which culminates in a lightning flash. This explanation, however, can hardly explain such high flash-rate convective systems that generate 150-200 flashes per minute as recorded by our cameras. Numerical simulations of charge separation processes and the resulting electrical field build-up cannot replicate such huge flash-rates by any of the known mechanism (see review in *MacGorman and Rust* (1998), chapter 6 *ibid.*).

Rather it seems that an intrinsic feedback mechanism, produced by the lightning fields` propagation and enhanced by the network morphology, leads to coherent pulsing which is observed as nearly simultaneous flashes. This synchronicity is dominated by the fastest oscillator (*Strogatz, 2001*), which in this case would be the thunderstorm cell with the highest flash rate. We plan to expand the present study to a larger data-set of lightning events recorded from space and by ground networks, which would allow us to better identify additional network features in large-scale storm systems.

References

- Albert, R., and A. L. Barabasi, 2002, Statistical Mechanics of Complex Networks: Review of Modern Physics, v. 74, p. 47-97.
- Atay, F. M., T. Biyikoglu, and J. Jost, 2005, Synchronization of Networks with Prescribed Degree Distribution: ArXiv:nlin.AO/0407024, v. v2.
- Boccippio, D. J., W. Koshak, R. Blakeslee, K. Driscoll, K. Mach, D. Buechler, W. Boeck, H. Christian, and S. J. Goodman, 2000, The Optical Transient Detector (OTD): instrument characteristics and cross-sensor validation: J. Atmos. Ocean Technol., v. 17, p. 441-458.
- Boeck, W. L., O. H. Vaughan Jr., R. J. Blakeslee, B. Vonnegut, and M. Brook, 1998, The role of the space shuttle videotapes in the discovery of sprites, jets and elves.: Jour. Atmos. Sol. Terr. Phys., v. 60, p. 669-677.
- Bollobas, B., 2001, Random Graphs: London, Academic Press.
- Erdos, P., and A. Renyi, 1960, On the Evolution of Random Graphs: Publ. Math. Inst. Hung. Acad. Sci., v. 5, p. 17-61.
- Füllekrug, M., 1995, Schumann resonances in magnetic field components.: Jour. Atmos. Terr. Phys., v. 57, p. 479-484.
- Israelevich, P., Y. Yair, A. D. Devir, J. H. Joseph, Z. Levin, I. Mayo, M. Moalem, C. Price, and A. Sternlieb, 2004, Transient airglow enhancement observed from the space shuttle Columbia during the MEIDEX sprite campaign.: Geophys. Res. Lett., v. 31.
- Kourtchatov, S. Y., V. V. Yu., V. V. Likhanskii, A. P. Napartovitch, F. T. Arecchi, and A. Lapucci, 1995, Theory of phase locking of globally coupled laser arrays.: Phys. Rev. A, v. 52, p. 4089-4094.
- Kuramoto, Y., 1984, Chemical Oscillations, Waves and Turbulence: Berlin, Springer.
- Lago-Fernandez, L. F., R. Huerta, F. Corbacho, and J. A. Siguenza, 2000, Fast Response and Temporal Coherent Oscillations in Small-World Networks: Physical Review Letters, v. 84, p. 2758-2761.
- Mazur, V., 1982, Associated Lightning Discharges: Geophys. Res. Lett., v. 9, p. 1227-1230.
- Molloy, M., and B. Reed, 1995, A Critical Point for Random Graphs with a Given Degree Sequence: Random Struct. Algorithms, v. 6, p. 161.
- NetMiner CYRAM Co. Ltd, 2004, NetMiner 2.5.
- Newman, M. E. J., 2003a, Random Graphs as Models of Networks, *in* S. Bornholdt, and H. G. Schuster, eds., Handbook of Graphs and Networks: Berlin, Wiley-VCH, p. 35-68.
- Newman, M. E. J., 2003b, The Structure and Function of Complex Networks: SIAM Review, v. 45, p. 167-256.
- Newman, M. E. J., S. H. Strogatz, and D. J. Watts, 2001, Random Graphs with Arbitrary Degree Distributions and Their Applications: Phys. Rev. E, v. 64, p. 026118.
- Pérez, C. J., A. Corral., A. Díaz-Guillera, K. Christensen, and A. Arenas, 1996, On self-organized criticality and synchronization in a lattice of coupled dynamical systems.: Int. J. Mod. Phys., v. B10, p. 1111-1151.
- Rakov, V. A., and M. A. Uman, 2003, Lightning: Physics and Effects: Cambridge, Cambridge University Press.

-
- Snijders, T. A. B., 1991, Enumeration and Simulation Methods for 0–1 Matrices with Given Marginals: *Psychometrika*, v. 56, p. 397-417.
- Strogatz, S. H., 2000, From Kuramoto to Crawford: exploring the onset of synchronization in populations of coupled oscillators.: *Physica*, v. D, p. 1-20.
- Strogatz, S. H., 2001, Exploring Complex Networks: *Nature*, v. 410, p. 268-276.
- Vonnegut, B., O. H. Vaughan Jr., M. Brook, and P. Krehbiel, 1985, Mesoscale observations of lightning from space shuttle.: *Bull. Am. Met. Soc.*, v. 66, p. 20-29.
- Wasserman, S., and K. Faust, 1994, *Social Network Analysis: Methods and Applications*: Cambridge, UK, Cambridge University Press.
- Watts, D. J., 1999, *Small Worlds: The Dynamics of Networks between Order and Randomness*: Princeton, NJ, Princeton Univ. Press.
- Watts, D. J., and S. H. Strogatz, 1998, Collective Dynamics of 'Small-World' Networks: *Nature*, v. 393, p. 440.
- Winfree, A. T., 1967, Biological rhythms and the behavior of populations of coupled oscillators: *J. Theor. Biol.*, v. 16, p. 15-42.
- Yair, Y., P. Israelevich, A. Devir, M. Moalem, C. Price, J. Joseph, Z. Levin, B. Ziv, and A. Teller, 2004, New sprites observations from the space shuttle: *J. Geophys. Res.*, v. 109, p. D15201/10.1029/2003JD004497.
- Yair, Y., C. Price, Z. Levin, J. Joseph, P. Israelevitch, A. D. Devir, M. Moalem, B. Ziv, and M. Asfur, 2003, Sprite observations from the space shuttle during the Mediterranean Israeli Dust Experiment (MEIDEX). *J. Atmos. Sol. Terr. Phys.*, v. 65, p. 635-642.
- Yair, Y., C. Price, B. Ziv, P. L. Israelevich, D. D. Sentamn, F. T. Sao-Sabbas, A. Devir, M. Sato, C. Rodger, M. Moalem, E. Greenberg, and O. Yaron, 2005, Space Shuttle observation of an unusual transient atmospheric emission: *Geophys. Res. Lett.*, v. 32, p. doi:10.1029/2004GL021551.
- Zipser, E. J., 1982, Use of a conceptual model of the life-cycle of mesoscale convective systems to improve very-short-range forecasts., *in* K. Browning, ed., *Nowcasting*: London, Academic Press, p. 191-204.

Acknowledgments

[1] This research is a fruit from the work of the crew of space shuttle Columbia: Rick Husband, William McCool, Michael Anderson, David Brown, Laurel Clark, Kalpana Chawla and Ilan Ramon.

[2] The MEIDEX was a joint project of the Israeli Space Agency and NASA. We wish to thank S. Janz and E. Hilsenrath of the Laboratory for Atmospheres at NASA/GSFC for their help in the calibrations of the Xybian cameras. Special thanks to the Hitchhiker team at NASA/GSFC: T. Dixon, M. Wright, K. Barthelme, S. Applebaum, C. Knapp, K. Harbert and to A. Lalich and T. Schneider, STS-107 flight planners at NASA/JSC, for making this experiment possible.

[3] This research was supported by the Israeli Science Foundation (ISF).

Tables

Table 1: Summary of the MEIDEX space shuttle video data used for the network analysis. MET is acronym to Mission Elapsed Time.

Orbit	MET	UT	Flash rate	Location
48	02/23:32:19 - 35:42	19.1.03 / 15:11:19 - 14:42	low	Indian Ocean
67	04/04:16:49 - 19:46	20.1.03 / 19:55:49 - 58:46	high	N. Australia
87 (1)	05/10:13:00 - 17:33	22.1.03 / 01:52:00 - 56:33	medium	Central Africa
87 (2)	05/11:21:38 - 28:49	22.1.03 / 03:00:38 - 07:49	Ext. high	S. America
162	10/02:38:18 - 42:14	26.1.03 / 18:17:18 - 22:14	high	N. Australia
239	14/21:52:22 - 55:46	31.1.03 / 13:31:22 - 34:46	medium	N. Australia

Figure Captions

Figure 1: Lightning activity observed over central Africa on January 22nd 2003. The diffused illumination of the clouds due to lightning flashes is clearly visible as elongated ellipses. The bright spot above the Earth's limb is the planet Saturn.

Figure 2: (a) Lightning sequence based on optical emissions detected by the MEIDEX camera from the high flash-rate storm, Orbit #67 (Pacific Ocean). The graph shows the number of active cells within a 1 s time window. (b) Fourier analysis of the flash clustering showing a maximum at 2.5 seconds between consecutive bursts of lightning activity.

Figure 3: Centrality Map of the lightning network of orbit 67, time-window 0.01 sec.

Figure 4: (a) The abundance of reciprocal and null dyads for the orbit 67 for 4 time-windows. (b) The abundance of null dyads for the same times.

Figure 5: Comparison between the observed values of the triad census for lightning network orbit 67 for 4 time-windows, with the predicted values of the two generalized random graph models.

Figure 6: Comparison of the observed values of the clustering coefficients of the lightning network of orbit 67 for 4 time-windows, with the expected values predicted by the random ER and the two generalized random graph models.

Figure 7: Comparison between the observed values of the average path length of the lightning network in the orbit 67 data, for 4 time-windows, with the predicted values of the ER model and the two generalized random graph models.

Figure 1

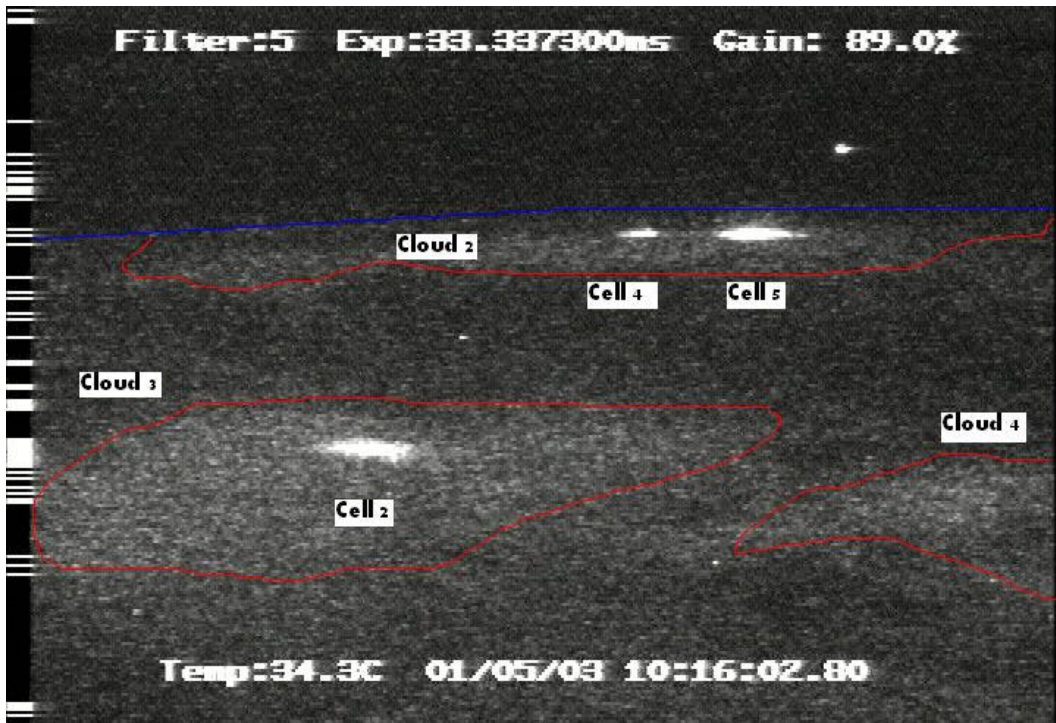


Figure2

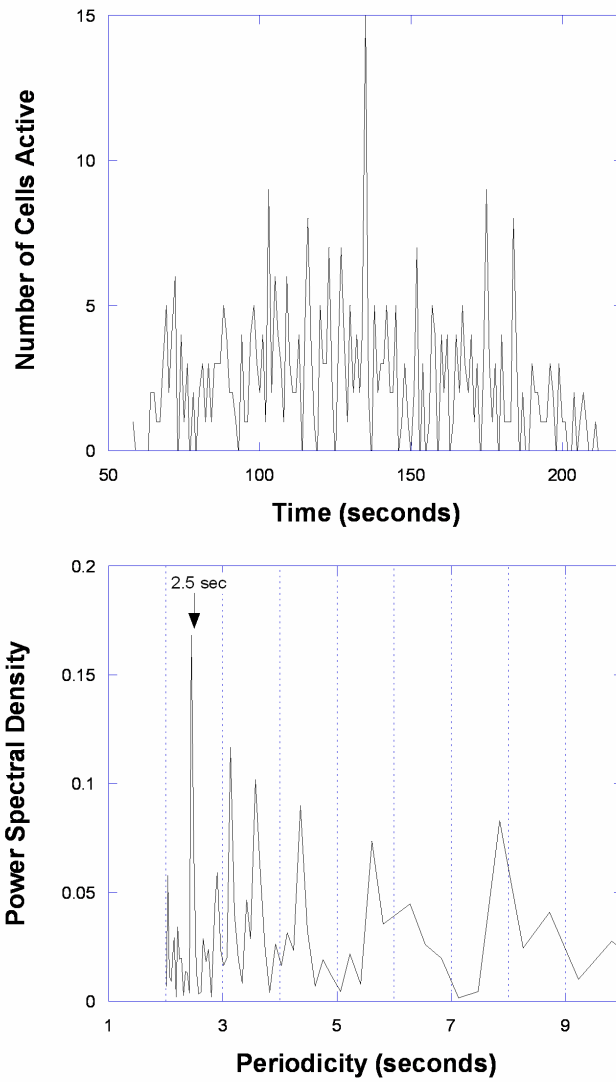


Figure 3

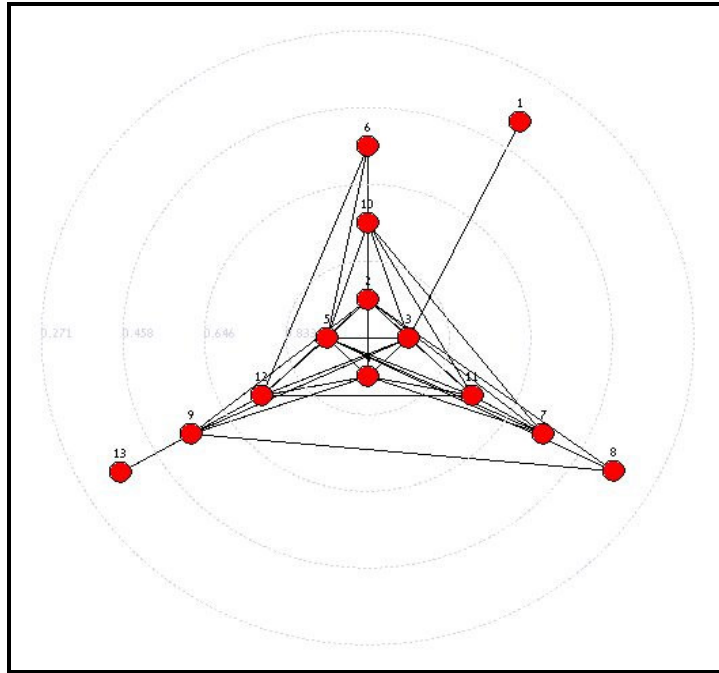


Figure 4a

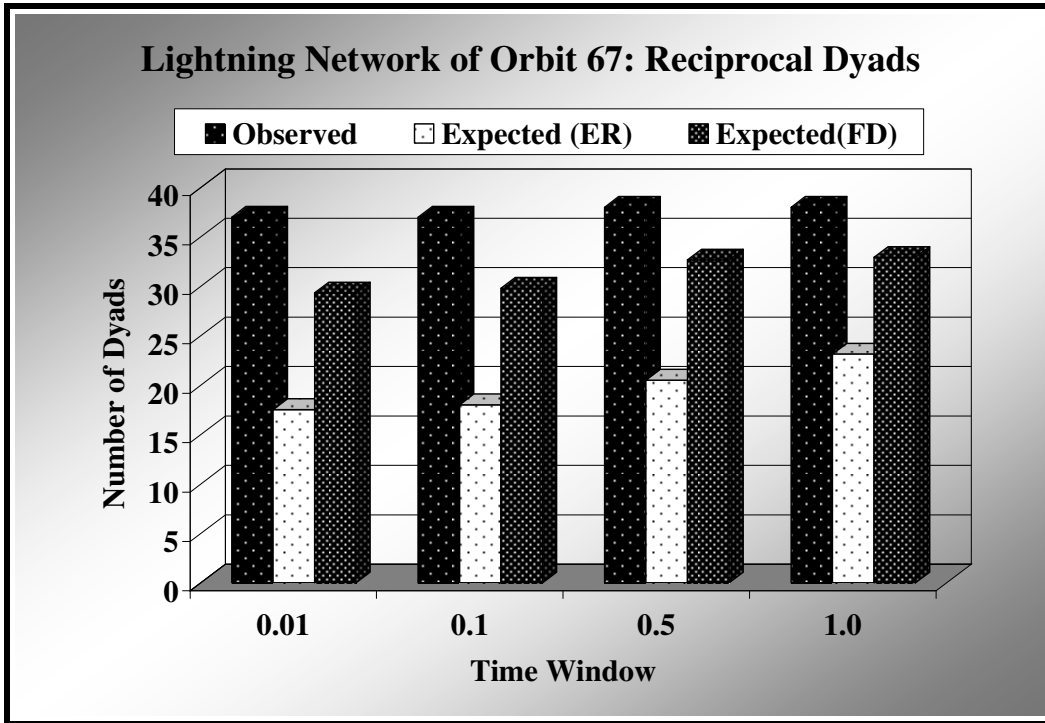


Figure 4b

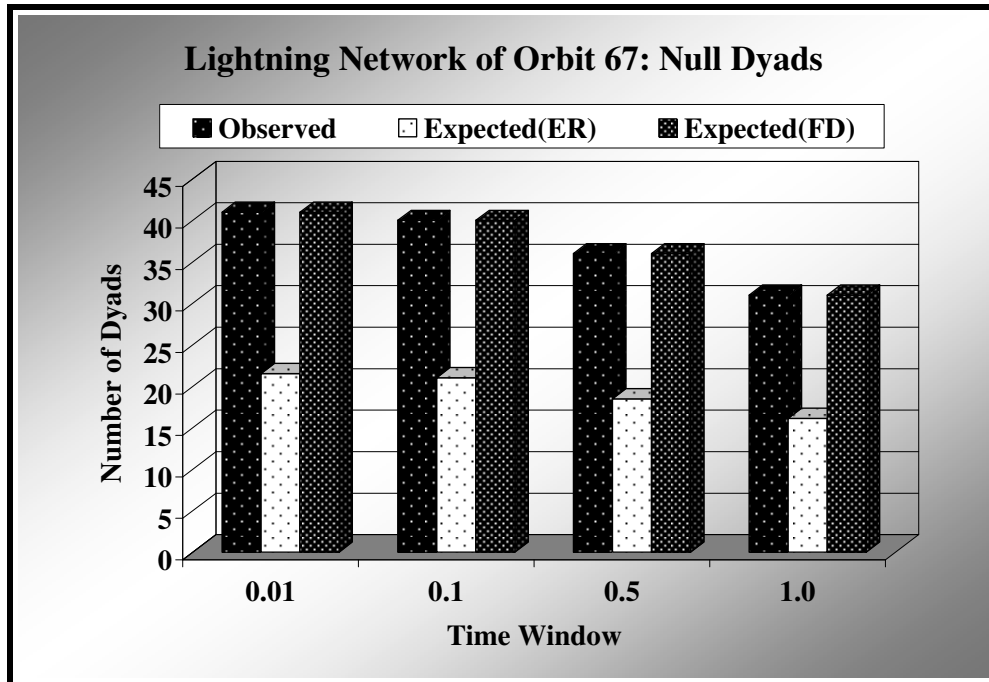


Figure 5

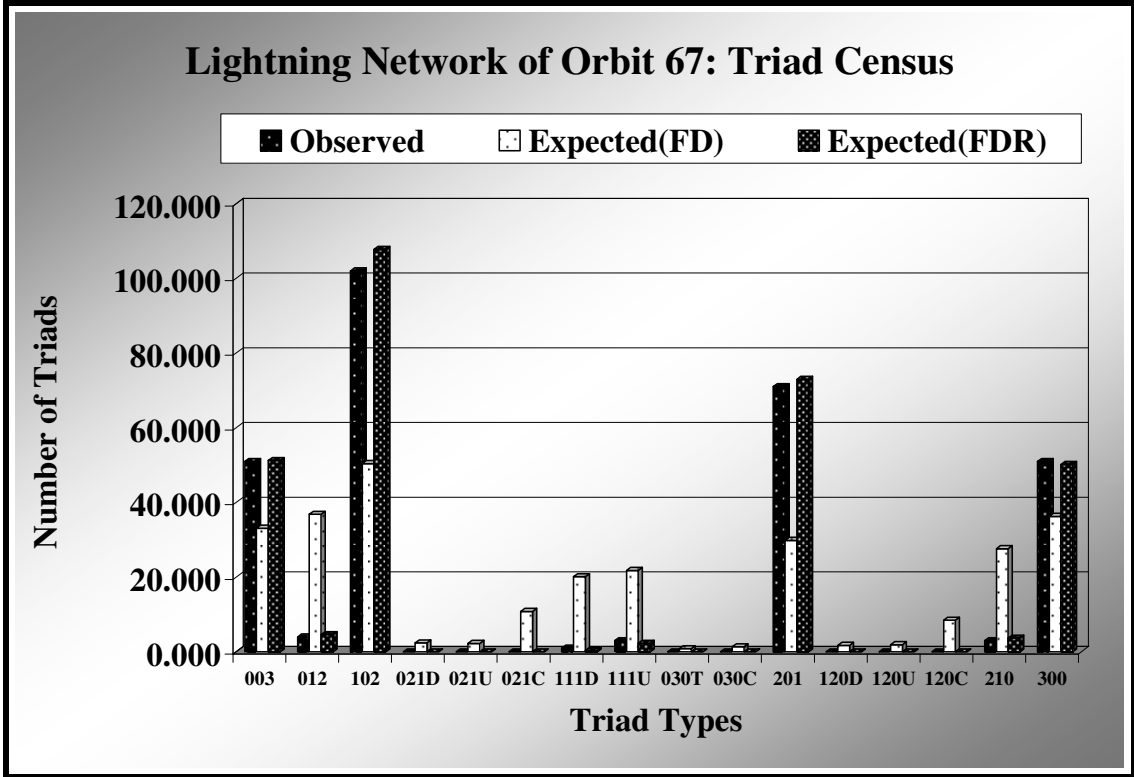


Figure 6

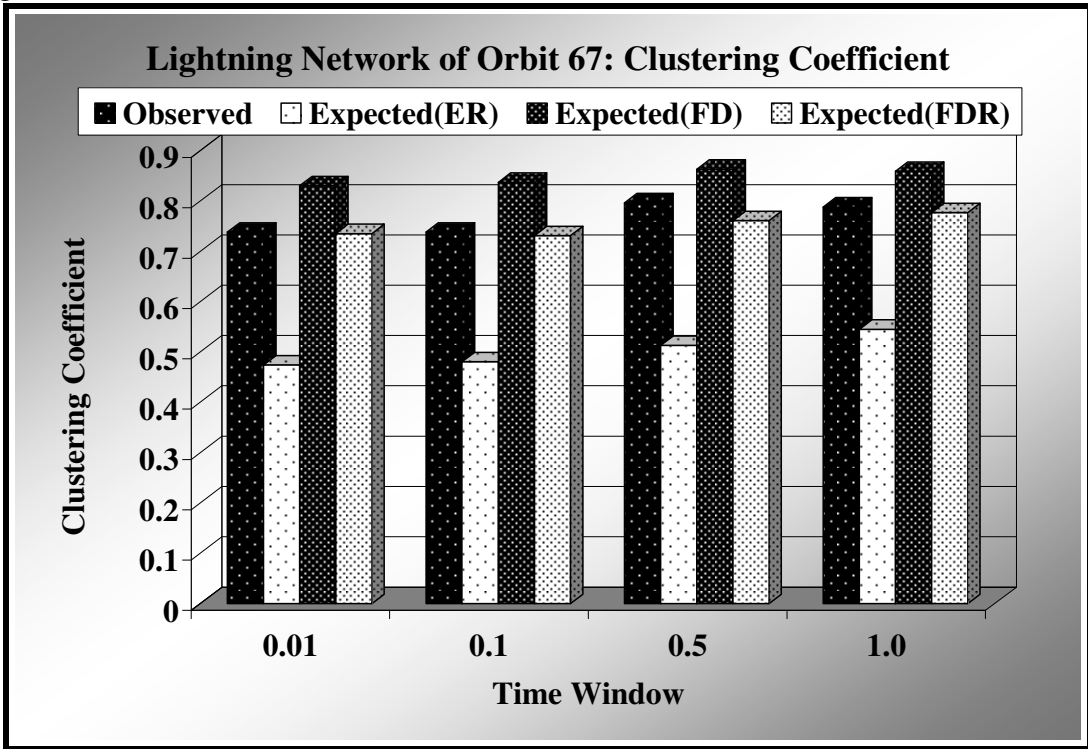


Figure 7

Lightning Network of Orbit 67: Average Shortest Path

